

**Natural Water Chemistry (Dissolved Organic Carbon, pH, and Hardness)  
Modulates Colloidal Stability, Dissolution, and Antimicrobial Activity of  
Citrate Functionalized Silver Nanoparticles**

**Supporting Information**

Lok R. Pokhrel<sup>1ac</sup>, Brajesh Dubey<sup>\*b</sup> and Phillip R. Scheuerman<sup>a</sup>

<sup>a</sup>Department of Environmental Health, College of Public Health, East Tennessee State  
University, Johnson City, TN 37614-1700, USA

<sup>b</sup>Environmental Engineering Program, School of Engineering, University of Guelph, 50 Stone  
Road West, Guelph, Ontario, Canada

<sup>c</sup>Current Address: US Environmental Protection Agency, National Health and Environmental  
Effects Research Laboratory, 200 SW 35<sup>th</sup> St., Corvallis, OR 97333, USA

Corresponding Author Tel: 001-519-824-4120 ext 52506; *E-mail*: [bdubey@uoguelph.ca](mailto:bdubey@uoguelph.ca)

**Total Pages: 12 (including cover page)**

**Total Figures: 6**

**Total Tables: 7**

**Citrate–AgNP Synthesis:** 1 mM AgNO<sub>3</sub> and 10 mM Sodium citrate dihydrate solutions were mixed together in a volume ratio of 2:1, respectively and the mixture was heated for 4 h at 70 °C using a water bath as previously described by El Badawy et al.<sup>1</sup>

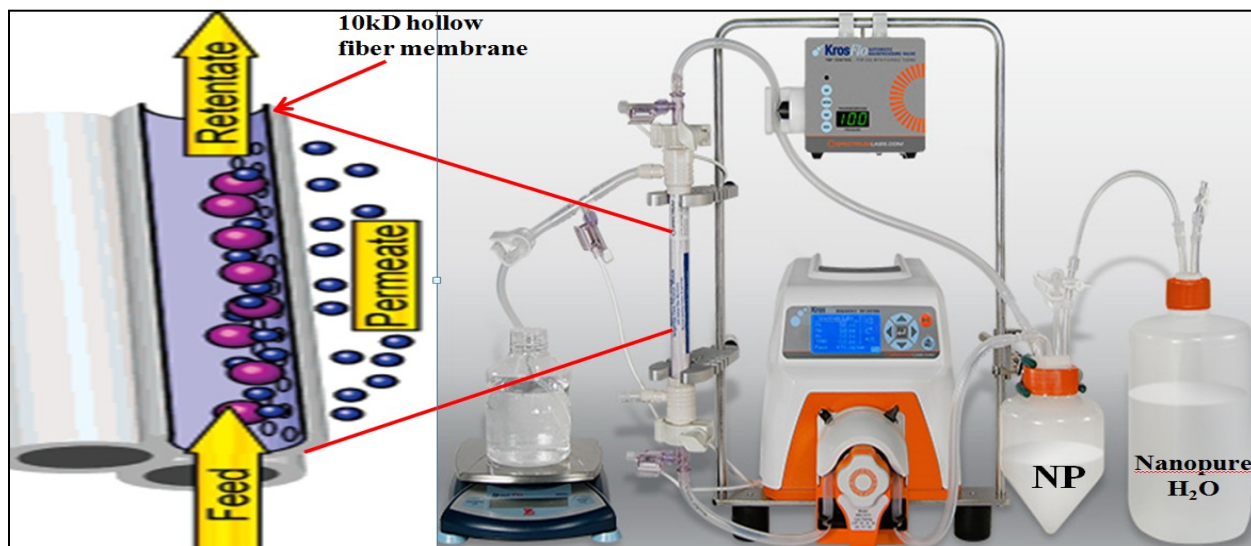


**Figure S1.** Photograph showing Kros *Flo* Research Ili Tangential Flow Filtration (TFF) System (right panel) equipped with 10 kD polysulfone hollow fiber diafiltration membranes (left panel) used for the purification of Citrate-AgNPs; adapted from <http://www.spectrumlabs.com/>; NP, nanoparticle suspension.

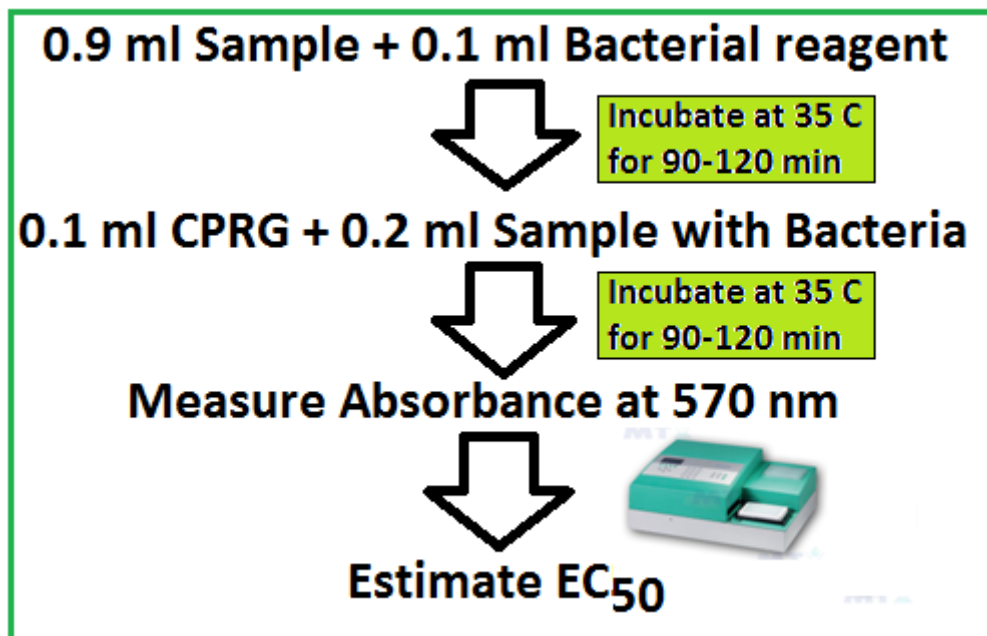


**Figure S2.** Schematic showing protocol for conducting  $\beta$ -Galactosidase bioassay using *E. coli* (Adapted from ref. 3); CPRG, Chlorophenol red galactopyranoside used as a substrate.

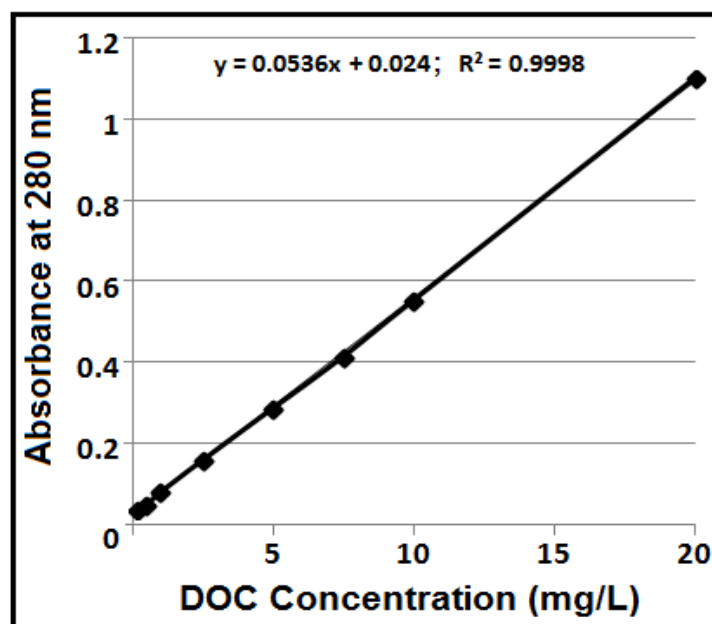


**Figure S3.** DOC calibration curve produced by UV-vis absorbance measurement at 280 nm and the concentrations were verified by persulfate-UV oxidation procedure.

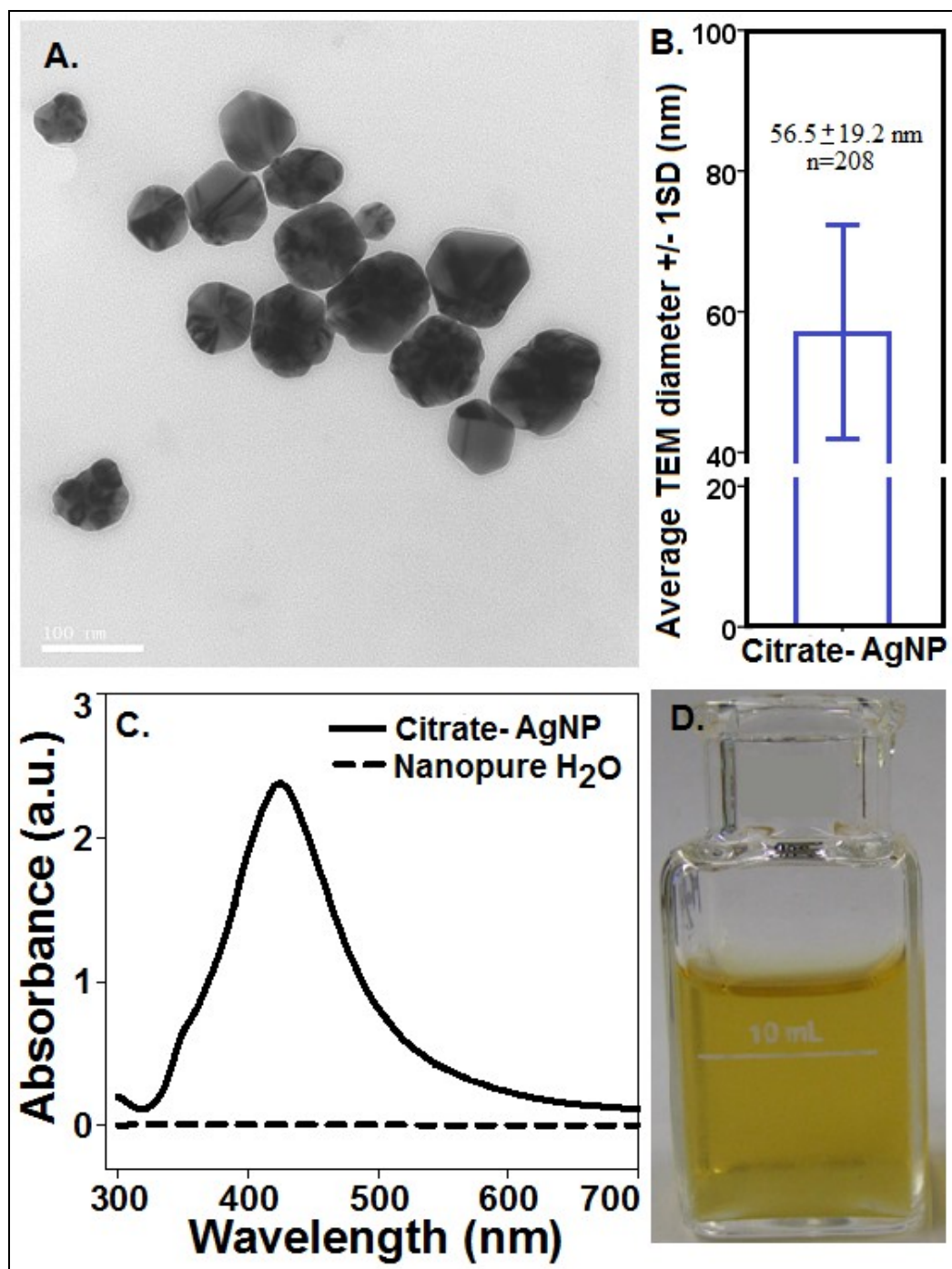


**Figure S2.** Representative TEM imagery (A), particle size distribution (B), surface Plasmon resonance spectrum (C), and stable colloidal suspension (D) of stock Citrate-AgNPs. Scale bar = 100 nm; n = number of particles analyzed from TEM images.

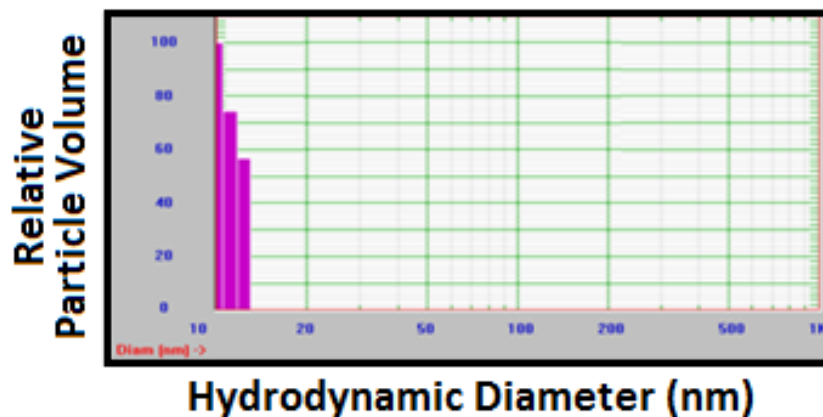


**Figure S1.** Particle size distribution (PSD) of Citrate-AgNPs in moderately hard water.

**Table S1.** Impact of moderately hard water (MHW) dilution of Citrate-AgNPs assessed by measuring average hydrodynamic diameters (HDD). Data show that dilution did not impact Citrate-AgNPs size in MHW as HDD remained unaltered with dilution.<sup>2</sup> SD, Standard deviation of the sample; X, dilution factor.

Dilution factor (v:v)	Citrate-AgNP	
	*HDD ± SD (nm)	% Volume
1X	11.0 ± 0.7	100
2X	10.9 ± 0.7	99.9
5X	11 ± 0.7	99.8
10X	11 ± 0.7	99.5
20X	10.9 ± 0.7	99.9

\* Volume weighted hydrodynamic diameter measured using DLS method.

**Table S2.** Purification protocol applied for cleaning as-synthesize Citrate-AgNPs using Tangential Flow Filtration (TFF) system.<sup>2</sup>

<b>Purification of unclean Citrate-nAg</b>	<b>Electrical Conductivity (<math>\mu\text{S}/\text{cm}</math>)</b>
Started Volume = 500 ml	1095
Ended Volume = 70 ml	1162
Volume increased to 500 ml by adding nanopure water	185
Ended Volume = 100 ml	283
Volume increased to 500 ml by adding nanopure water	36
Ended Volume = 75 ml	68
Volume increased to 500 ml by adding nanopure water	11
Ended Volume = 150 ml	20
Volume increased to 500 ml	5*

\* obtained as clean Citrate-AgNP suspension with electrical conductivity 5  $\mu\text{S}/\text{cm}$ .

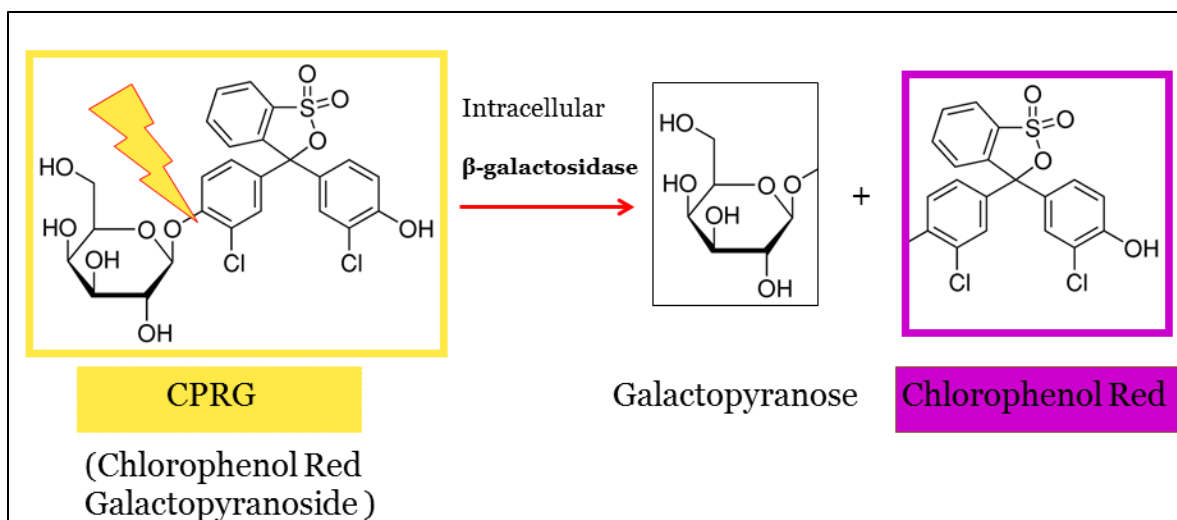


**Figure S5.** Mechanism of intracellular  $\beta$ -Galactosidase mediated conversion of chlorophenol red galactopyranoside (CPRG used as a substrate; yellow color) into chlorophenol red (magenta color) which is quantified at 570 nm using a microplate reader (quoted from our previous publication).<sup>2</sup>

**QA/QC.** All containers used for this study were soaked in 5%  $\text{HNO}_3$  overnight, cleaned several times using nanopure water (resistance = 18.3  $\text{M}\Omega\text{-cm}$ ), and air dried before use. Typical metal analysis using an Atomic Absorption Spectroscopy (AAS)-Flame/Furnace comprised of the method blank, digested samples, sample duplicate, spiked sample, and appropriate internal standards. The rinse blank consisting of 2%  $\text{HNO}_3$  made in nanopure water was used to clean the system following analysis of every ten samples. Maintenance of AAS is routinely performed through permanent maintenance contract with the manufacturer. Five-point calibration curves were typically developed for Ag analysis with AAS.

**Table S3.** Generalized Linear Model and parameter estimates showing main effects of HDD, zeta potential and Ag dissociation rate % under variable dissolved organic carbon (DOC) concentrations and their interactive effects on the toxicity of Citrate-AgNPs (used as EC<sub>50</sub> values for β-Gal bioassay under a range of DOC concentrations, a dependent variable in the model). Model deviance value was compared with the other models to test the goodness of fit of the model presented based on information criteria that small-is-better.

<b>Dependent variable: EC<sub>50</sub> (DOC)</b>	<b>Likelihood Ratio</b>	<b>df</b>	<b><i>p</i></b>	
<b>Source</b>	<b>Chi-Square</b>			
Model	59.137	4	< 10E-6	
HDD	8.487	1	< 0.005	
Zeta Potential	6.311	1	< 0.05	
Ag Dissociation Rate %	16.102	1	< 10E-4	
HDD x Zeta Potential x Ag Dissociation Rate %	6.498	1	< 0.05	

<b>Parameter</b>	<b>Coefficient B</b>	<b>Std Error</b>	<b>Wald Chi- Square (df)</b>	<b><i>p</i></b>
HDD	0.157	0.0464	11.413 (1)	< 0.005
Zeta Potential	-0.25	0.0894	7.846 (1)	<0.01
Ag Dissociation Rate %	2.815	0.5237	28.883 (1)	<10E-6
HDD x Zeta Potential x Ag Dissociation Rate %	0.005	0.0017	8.132 (1)	< 0.005



**Table S4.** Generalized Linear Model and parameter estimates showing main effects of HDD under variable pH and the interactive effects of HDD, zeta potential and Ag dissociation rate % on the toxicity of Citrate-AgNPs (used as  $EC_{50(pH)}$  values for  $\beta$ -Gal bioassay under variable pH, a dependent variable in the model). Model deviance value was compared with the other models to test the goodness of fit of the final model based on the information criteria that small-is-better.

<b>Dependent variable: <math>EC_{50(pH)}</math></b>	<b>Likelihood Ratio</b>	<b>df</b>	<b><i>p</i></b>	
<b>Source</b>	<b>Chi-Square</b>			
Model	42.479	4	< 10E-6	
HDD	9.355	1	< 0.005	
HDD x Zeta Potential	7.393	1	< 0.01	
HDD x Ag Dissociation Rate %	5.718	1	< 0.05	
HDD x Zeta Potential x Ag Dissociation Rate %	4.672	1	< 0.05	

<b>Parameter</b>	<b>Coefficient B</b>	<b>Std Error</b>	<b>Wald Chi-Square (df)</b>	<b><i>p</i></b>
HDD	10.995	2.9214	14.166 (1)	< 10E-6
HDD x Zeta Potential	0.819	0.2562	10.220 (1)	< 0.005
HDD x Ag Dissociation Rate %	-8.992	3.3225	7.324 (1)	< 0.01
HDD x Zeta Potential x Ag Dissociation Rate %	-0.691	0.2892	5.713 (1)	< 0.05

**Table S5.** Generalized Linear Model and parameter estimates showing main effects of Ag dissociation rate % under variable hardness conditions on the toxicity of Citrate-AgNPs (used as  $EC_{50}(\text{Hardness})$  values for  $\beta$ -Gal bioassay under variable hardness, a dependent variable in the model). Model deviance value was compared with the other models to test the goodness of fit of the model presented based on information criteria that small-is-better.

<b>Dependent variable:</b>	<b>Likelihood Ratio</b>	<b>df</b>	<b><i>p</i></b>	
$EC_{50}(\text{Hardness})$	<b>Chi-Square</b>			
<b>Source</b>				
Model	39.604	3	< 10E-6	
HDD	6.003	1	< 0.05	
Ag Dissociation Rate %	18.567	1	< 10E-4	
HDD x Zeta Potential x Ag	5.711	1	< 0.05	
Dissociation Rate %				
<b>Parameter</b>	<b>Coefficient B</b>	<b>Std</b>	<b>Wald Chi-</b>	<b><i>p</i></b>
		<b>Error</b>	<b>Square (df)</b>	
HDD	-0.621	0.2223	7.789 (1)	0.005
Ag Dissociation Rate %	32.049	4.8108	44.380 (1)	< 10E-4
HDD x Zeta Potential x Ag	-0.057	0.0210	7.313 (1)	< 0.01
Dissociation Rate %				

**Table S6.** Comparison of the Generalized Linear Model (GLM)-predicted toxicity ( $EC_{50}$ ) versus experimentally-derived toxicity of Citrate-coated AgNPs in *Escherichia coli*.

Citrate-AgNP		$\beta$ -Galactosidase activity in <i>Escherichia coli</i>		
		Experimental $EC_{50} \pm S.D.$ (mg/L)	GLM-Predicted	
			$EC_{50}$ (mg/L)	% Precision
<b>DOC (mg/L)</b>	0	5.79±2.87	5.68	98.1
	2	8.56±0.24	8.66	101.1
	5	11.55±0.35	11.71	101.4
	10	13.28±0.50	11.72	88.3
	20	13.38±0.62	14.10	105.4
<b>pH</b>	5	2.65±0.53	2.01	75.8
	6	3.33±0.28	3.50	105.1
	7	8.56±0.24	9.62	112.4
	7.5	36.7±3.33	35.46	96.6
<b>Hardness (mg/L as CaCO<sub>3</sub>)</b>	150	37.6±3.03	34.98	93.0
	200	11.78±0.5	17.52	148.7
	250	11.4±1.49	11.61	101.7
	280	8.56±0.24	5.24	61.2

GLM, Generalized Linear Model; % Precision = 100(GLM Predicted  $EC_{50}$ /Experimental  $EC_{50}$ ). Citrate-AgNP, Citrate-coated AgNP.

**Table S7.** Physicochemical characteristics of the water samples collected from the Watauga River, Elizabethton, TN (36.3339 °N, -82.2704 °W).

<b>Date Sampled</b>	<b>pH</b>	<b>Temperature (°C)</b>	<b>Electrical Conductivity (µS/cm)</b>	<b>Dissolved Oxygen (mg/L)</b>	<b>Hardness (mg/L as CaCO<sub>3</sub>)</b>	<b>Alkalinity (mg/L as CaCO<sub>3</sub>)</b>	<b>NH<sub>3</sub>-N<sub>2</sub> (mg/L)</b>	<b>Dissolved Organic Carbon (mg/L)</b>	<b>Total Ag (µg/L)</b>
3/30/2012	7.3	6.7	98.5	8.1	316.5	39	0.02	1.87	bdl
5/30/2012	6.6	13	96	8.0	318.5	31	0.02	1.96	bdl
7/27/2012	7.1	17	112.5	8.0	306	44	0.02	2.07	bdl
9/28/2012	7.0	19	119	8.3	311	45.5	0.02	2.08	bdl

Reported values are the means of the duplicate samples; bdl denotes below detection limit of the Graphite Furnace-AAS; detection limit for Ag was 0.54 µg/L; pH, temperature, electrical conductivity, and dissolved oxygen were measured by Hanna Instruments multiparameter meter 9828 (Hanna Instruments, Michigan); hardness (method 10247), alkalinity (method 8203) and NH<sub>3</sub>-N<sub>2</sub> (method 8038) were measured using the standard Hach methods; dissolved organic carbon was verified following the method SM 5310C coupled with persulfate-UV oxidation procedure.

### References Cited in Supporting Information

1. A. M. El Badawy, T. P. Luxton, R. G. Silva, K. G. Scheckel, M. T. Suidan and T. M. Tolaymat. *Environ. Sci. Technol.*, 2010, **44**, 1260–1266
2. L. R. Pokhrel, B. Dubey, T. Silva, A. M. El Badawy, T.M. Tolaymat and P. R. Scheuerman, *Sci. Total Environ.*, 2012, **426**, 414–422.
3. G. Bitton, K. Jung and B. Koopman, *Arch. Environ. Contam. Toxicol.*, 1994, **27**, 25–28.